Int J Adv Manuf Technol manuscript No.
(will be inserted by the editor)

Modelling of segmentation-driven vibration in machining

Chris M Taylor · Sam Turner · Evangelos Papatheou · Neil D Sims

Submitted: 28 November 2011

Abstract Excessive vibration, such as chatter, is a common problem in machining processes. Meanwhile, numerous hard, brittle metals have been shown to form segmented chips, also known as sawtooth chips, during machining. In the literature, a cyclic cutting force has been demonstrated where segmented chips are formed, with the force cycle corresponding to the formation of segments. Segmented chip formation has been shown to be linked to high vibration levels in turning and milling processes. Additionally, it has been proposed that the amplitude of chatter vibrations can be limited by interference between the tool flank and wavy workpiece surface, a phenomenon known as tool flank process damping.

In this contribution, a model is proposed to predict the amplitude of forced vibration arising due to the formation of segmented chips during turning. The amplitude of vibration was calculated as a function of cutting parameters. It was demonstrated that the model can be extended to account for the effect of tool flank process damping. For validation, titanium Ti6Al4V alloy was turned using a flexible toolholder, with surface speed ranging from 10 to 160m/min, feedrate from 0.1 to 0.7mm/rev and width of cut from 0.35 to 4mm.

In the experimental validation, 25 of 68 test cuts exhibited high amplitude vibration. In 16 of these cases, the main cause was concluded to be chip segmentation, which can be predicted by the model. The model is thus considered of practical value to machinists.

Chris M Taylor
Dept of Mechanical Engineering, University of Sheffield, Mappin Street, S1 3JD, UK
Tel.: +44 114 222 9588
E-mail: c.taylor@amrc.co.uk
Present address: AMRC with Boeing, The University of Sheffield, Advanced Manufacturing Park, Wallis Way, Catcliffe, Rotherham S10 1GZ, UK

Sam Turner
AMRC with Boeing, The University of Sheffield, Advanced Manufacturing Park, Wallis Way, Catcliffe, Rotherham S10 1GZ, UK

Evangelos Papatheou
Dept of Mechanical Engineering, University of Sheffield, Mappin Street, S1 3JD, UK

Neil D Sims
Dept of Mechanical Engineering, University of Sheffield, Mappin Street, S1 3JD, UK,
Tel.: +44 114 2227724
Fax.: +44 114 2227890
E-mail: n.sims@sheffield.ac.uk

Keywords chatter · segmentation · process damping · titanium

1 Introduction and background literature

Excessive vibrations during machining can lead to a poor surface finish, increased tool wear, reduced machine life, and limited productivity. Consequently, there has been a great deal of research over the years to understand, predict and mitigate machining vibrations. Much of this work has focussed on regenerative chatter, which is arguably the most common problem in practice. However, the present contribution is related to improving the understanding and prediction of a type of machining vibration which corresponds to the formation of segmented chips. To begin, the relevant literature is reviewed, and the aims of this paper are then explained in the context of previous published work.

1.1 Machining vibrations

One of the most common forms of machining vibration is regenerative chatter, caused by unstable self-excited vibrations between the cutting tool and workpiece [1,2]. This vibration is particularly relevant at high cutting speeds. However, hard-to-cut materials such as titanium alloys exhibit high chemical reactivity and low thermal conductivity [3], so they must be processed at lower cutting speeds to minimise tool wear. At these lower cutting speeds a phenomenon known as process damping increases regenerative chatter stability. Process damping is said to be caused by interaction of the machined-surface wave pattern and the flank of the cutting tool, described further in Tlusty's book [2]. Recently, there have been many studies to predict the increased stability due to process damping [4,5,6,7], but one of the earliest studies was the work of Hooke and Tobias [8]. They described the maximum amplitude of vibration, a_{max}, for a sharp tool cutting a wavy workpiece, assuming a sinusoidal vibration with no interference between the tool flank and workpiece:

$$a_{max} = \frac{V \tan(\alpha)}{60\omega_c} \tag{1}$$

Here α is the tool relief angle, ω_c is the frequency of vibrations, and V is the turning surface speed in m/min. The frequency of vibrations ω_c is the frequency of regenerative chatter vibrations, and so Eq. (1) shows the relationship between the process damping phenomenon and regenerative chatter. However, this assumes that there is no interference or ploughing between the workpiece and tool [9], and consequently Eq. (1) can only be used to give an approximate indication of the process-damped vibration amplitude.

Nevertheless, there are some scenarios where machining vibration is not dominated by regenerative chatter or the associated process damping phenomenon, but is caused directly by the chip formation forces. Consequently the relevant literature concerning chip formation will now be reviewed.

1.2 Chip formation effects

Vyas and Shaw [10] defined five types of chips occurring in metal cutting. These are (1) steady-state continuous chips, (2) wavy chips, (3) built-up edge chips, (4) discontinuous chips and (5) sawtooth chips. As the

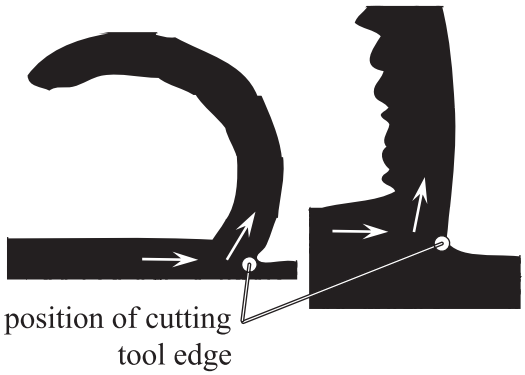

Fig. 1 Schematic views of steady-state continuous chip formation, left, and segmented chip formation, right

name implies, chip type (1) gives rise to cutting conditions with minimal disturbances. Such a chip is found in the cutting of ductile workpiece materials [11]. An example of a steady-state continuous chip is shown on the left hand side of Fig. 1. At the opposite extreme to chip type (1), discontinuous chips crack during cutting, forming sections which may or may not be bonded together. Brittle materials and materials with hard inclusions or impurities form discontinuous chips when cut [11]. Sawtooth chips are recognisable by the formation of sharp points on the free surface. Materials forming sawtooth chips are also relatively hard and brittle. Additionally, the properties of low thermal conductivity and thermal softening make materials susceptible to sawtooth chip formation. A notable example is titanium alloy. The formation of sawtooth segments is initiated by cracking, and aided in part by highly-localised adiabatic shear [10]. Some authors refer to sawtooth chips as segmented or serrated chips. The term segmentation (meaning the formation of sawtooth chips) is used in this work. An example of a sawtooth, or segmented, chip is shown on the right hand side of Fig. 1.

The vibration-inducing nature of segmented and discontinuous chip formation has been recognised for many years, an early example being the work by Cook [12]. In another early example, Landberg [13] studied the turning of carbon steel and brass. The frequency of chip segment formation was predicted as a function of parameters including surface speed. Comparison with experiment showed that the frequency of dominant vibrations as measured on the cutting tool was within a few percent of the predicted segmentation frequency when cutting brass, with predictions being less accurate for the steel. Strong vibrations were reported where the segmentation frequency was close to the natural frequency of a structural component in the cutting system. This forced vibration was said to lead to roughness of the cut surface. A study by Jeelani and Ramakrishnan [14] proposed that chip formation had a pronounced effect on the workpiece surface finish, when turning the alloy Ti6Al2Sn4Zr2Mo.

Bayoumi and Xie's data [15] showed that in turning of Ti6Al4V, the length of segments formed was approximately proportional to the experimental feedrate. Surface speed was seen to have a less significant effect on segment length. Komanduri and Von Turkovich [3] recorded images of chip formation for titanium Ti6Al4V alloy, and described the stages of segment formation. Cutting forces and the velocity of the chip relative to the tool were said to oscillate significantly as segments formed. Molinari *et. al* [16] showed

amongst their other findings that for Ti6Al4V alloy, segmented chips formed at all surface speeds tested, including speeds way in excess of 1000m/min. The uncut chip thickness was either 0.12 or 0.25mm in the experiments performed.

Nurul Amin *et al*. [17] investigated the effect of segmented chip formation on vibration in end milling. Ti6Al4V was end milled with feed 0.1mm/tooth and surface speed between 40 and 250m/min. Frequency analysis of acceleration data showed that the tool, spindle, or both were excited to vibrate at high amplitude during cutting, depending on the insert type and the surface speed during the cut. The evidence gathered by Nurul Amin *et al*. points to the importance of segmentation-driven vibration in this particular milling case. Sun *et al*. [18] conducted research in turning of Ti6Al4V, finding that the frequency of oscillation of the cutting force at feedrates equal to or greater than 0.149mm/rev was proportional to surface speed, inversely proportional to the feedrate and independent of width of cut. The cyclic fluctuation in cutting force was said to be caused by the segmented chip formation process. Both Nurul Amin *et al*. and Sun *et al*. discussed excitation of vibration of a significant amplitude where the segmentation frequency was close to some integer multiple of the first vibration mode of the system. Nurul Amin *et al.* found that segmentation at frequencies up to four times the first mode of a structural element could cause excessive vibration of that element.

Doi and Ohhashi [19] took a modelling approach to the prediction of chip segmentation-driven vibration in turning of two steels. The approach was based on parametric rather than forced excitation, using the Mathieu equation to predict unstable cutting conditions. The model correctly identified surface speeds where vibration levels were unusually high. Morehead *et al.* [20] also investigated segmented chip formation during turning of steels.

Most recently, the authors of the current work analysed the frequency and amplitude of vibrations measured in turning of Ti6A4V alloy [4], to investigate the mechanisms of vibration excitation. A chip delay effect model was developed [21], and the workpiece surface slope was calculated to analyse process damping at low speed. The authors concluded that chip segmentation could play an important role in exciting vibration, and was deserving of further investigation.

1.3 Summary and aims for study

The literature to date shows that both regenerative chatter and chip formation mechanisms can lead to significant vibration levels in turning and milling processes. Much of the research to date regarding vibration driven by chip segmentation has been observational in nature. Although segmentation-driven vibration has been observed in the cutting of titanium alloys, modelling of vibration driven by chip segmentation has received little attention relative to the development of regenerative vibration theory. No process map has yet been created for forced vibration driven by chip segmentation. Therefore, the aims in performing this study were to:

1. Develop a quantitative model of forced vibration arising due to the chip segmentation phenomenon in machining.
2. Validate the above model by comparing model-derived vibration levels against experimentally-derived vibration data, as a function of cutting parameters.
3. As part of the validation process, use frequency domain methods to distinguish between the occurrence of segmentation-driven vibration and regenerative chatter in experimental results.
4. Identify the conditions for process damping in the case of vibration driven by chip segmentation.

2 Theory

In this section, a basic model is developed to predict the amplitude of vibrations that are caused by chip segmentation. In addition, a method for predicting the influence of process damping is briefly summarised, since process damping is likely to limit the amplitude of these vibrations.

2.1 Segmentation-driven vibration amplitude

The model aims to predict the amplitude of forced vibration due to chip segmentation during turning. Consequently the following assumptions are made:

a) The cutting system is equivalent to an open loop block system (i.e. no regenerative effect), with the cutting force as input and tool displacement as output.
b) Linear vibration in the feed direction x is considered. Nonlinearities due to variation of specific cutting force with uncut chip thickness, and variation of tool stiffness and damping with displacement, are not considered. The tool does not leave the cut due to vibration.
c) The cutting force oscillates sinusoidally around a mean value, at the frequency of the chip segmentation.
d) All chip segments are assumed uniform in length, so the segmentation frequency takes a single value.

For this cutting system, a linear relationship would be expected between the amplitude of cutting force oscillation and the amplitude of vibration, for a given segmentation frequency. Having no feedback means that the effect of the previously-cut surface is not considered by the model.

The starting point for the model is the empirical data from the literature [15,17,18], which leads to a relationship between the cutting surface speed V, feedrate s, width of cut b, and segmentation frequency:

$$\omega_{seg} = f(V,s,b) \tag{2}$$

Meanwhile, the segmentation wavelength λ is based on a well-known relationship:

$$\lambda = \frac{2\pi V}{\omega_{seg}} \tag{3}$$

which is related to the spacing between the segments on the chip. As an approximation, the frequency is assumed to be insensitive to the width of cut, and the segmentation wavelength is proportional to the feed

rate or chip thickness, giving:

$$\omega_{seg} = \frac{2\pi V}{60\lambda_0 s} \tag{4}$$

Here, ω_{seg} has units of rad/s, V has units of m/min, and s has units of m/rev. The term λ_0 is an empirical dimensionless parameter referred to as the segmentation wavelength coefficient, which relates the physical segmentation wavelength to the feed rate or chip thickness:

$$\lambda = \lambda_0 s \tag{5}$$

Just like the classical 'specific cutting force' K [2], the segmentation wavelength coefficient is an empirical value for a given workpiece and tool combination.

With reference to assumption (c), the cutting force is of the form:

$$f_x(t) = \bar{f}_x + \Delta f_x \sin(\omega_{seg} t) \tag{6}$$

where $\bar{f}_x$ is the mean cutting force and Δf_x is the peak amplitude of the periodic cutting force. The accurate measurement of the dynamic cutting forces due to segmentation can be difficult. In the absence of such data, the periodic component of the cutting force is assumed to be proportional to the mean cutting force, i.e.:

$$\Delta f_x \approx \frac{\bar{f}_x}{n} \tag{7}$$

Here, n is a calibration constant that accounts for the true amplitude of the periodic cutting force at the segmentation frequency. The mean cutting force is obtained using the standard specific cutting force [2]:

$$\bar{f}_x = K(V) b s \tag{8}$$

where K is the specific cutting force (in the direction normal to the surface) that is allowed to be an empirical function of the surface speed V. Since the case of forced vibration is assumed, the amplitude of motion can therefore be written as:

$$a_x = G(\omega_{seg}) \Delta f_x(V, s, b) \tag{9}$$

where $G(\omega)$ is the frequency response function (FRF) of the flexible structure in the feed direction. Substituting Eq. (4), Eq. (7), and Eq. (8) into Eq. (9) leads to:

$$a_x = G\left(\frac{2\pi V}{60\lambda_0 s}\right) \frac{K(V) b s}{n} \tag{10}$$

Consequently the amplitude of vibration can be predicted based upon the cutting conditions (V, b, s) and the following empirical data:

1. The segmentation wavelength coefficient, λ_0
2. The calibration constant, n
3. The measured frequency response function, $G(\omega)$
4. The specific cutting force versus surface speed, $K(V)$

Here, data requirements (3) and (4) are equivalent to the data used for traditional chatter stability analysis. (1) and (2) are new empirical relationships, which (as for (3) and (4)) must be obtained for particular workpiece materials and tools.

2.2 Tool-flank rubbing

In practice, the amplitude of segmentation-driven vibration will be limited due to the onset of interference between the tool flank and the workpiece. This interference is similar to the process damping mechanisms described in the literature, except that the cause of the vibrations is the oscillating chip generation force rather than the regenerative effect.

It transpires that the model of Hooke and Tobias [8] (Eq. (1)) can be directly applied if the chatter frequency ω_c is replaced by the segmentation frequency ω_{seg}:

$$a_{max} = \frac{V \tan(\alpha)}{60\omega_{seg}} \tag{11}$$

Substituting Eq. (4) into Eq. (11):

$$a_{\max} = \frac{s\lambda_0 \tan(\alpha)}{2\pi} \tag{12}$$

Recall that λ_0 is the (empirical & dimensionless) segmentation wavelength coefficient, and α is the tool relief angle. This means that the process damped vibration amplitude limit is independent of surface speed, and proportional to the feed, for vibration driven directly by chip segmentation forces.

3 Experimental setup

The aim of this section is to describe two experiments: one designed to obtain the empirical constants (segmentation wavelength coefficient λ_0, specific cutting force K, and calibration constant n), and one designed to test the model proposed by Eq. (10) and (12).

3.1 Workpiece, tooling and instrumentation specifications

The machine used in most of the cutting tests was a MAG Cincinnati Hawk 300 NC lathe. Some additional tests were performed on a manual lathe, described in Section 3.2. Tests were conducted without coolant, allowing the cutting process to be monitored visually. All data was acquired using a four-channel Spectral Dynamics SigLab system, with a sampling frequency up to 51.2kHz.

The workpiece was a 150mm diameter bar of annealed titanium Ti6Al4V alloy. The bar's constituents, heat treatment and basic properties can be found in Table 1. Cutting was performed with grade H13A uncoated carbide Sandvik Coromant inserts. These were supplied with blank N123K2-0720-0002-BG geometry, then rake and relief angles were applied by optical profile grinding. The rake angle was 7° in most

C	Si	Mn	Mo	Ti	Al	V	Fe	Cu
0.010	<0.01	<0.01	<0.01	Bal.	6.41	4.08	0.15	0.02
B	Zr	Y	O	N	Sn	Cr	Ni	H
< 0.001	<0.01	< 0.001	0.18	0.007	<0.01	<0.01	<0.01	.0014
Heat treatment: 704°C for one hour								
UTS: 945 MPa								
Hardness: 33HRC								

Table 1 Percentage constituents of titanium 6-4 workpiece, supplied by Maher Ltd, UK.

cases, although 0°, 10°, and 15°, angles were tried in additional tests. Relief angles specified were 3.5° and 7°. Profilometry confirmed the ground angles to be within 0.3° of the nominal value. The tool edge condition was sharp.

The operating frequency range of the measurement transducers is now considered. This is particularly important for segmentation-driven vibration, as the segmentation frequency varies over such a large range. The modal testing hammer used had an upper frequency limit of 9.5kHz, while the accelerometers gave their most accurate response up to 10kHz with a reasonably accurate response at up to 25kHz. The displacement probe had an operating limit of 10kHz. These transducers are all fit for purpose regarding operating frequency range. For the dynamometer used in cutting force tests, modal testing showed that the dynamometer and toolholder combination used had a first and second mode of vibration at 1160 and 3400Hz. Consequently the frequency and amplitude of periodic forces (due to chip segmentation) may be difficult to measure.

3.2 Empirical calibration measurements

To determine the required empirical data (specific cutting force versus surface speed, and the amplitude and frequency of cutting force oscillations), a series of rings was created and cut orthogonally. The 7° rake and 7° relief angle inserts described above were held in a high-stiffness toolholder, which was mounted in a Kistler 9121 dynamometer fitted with a machine VDI interface. Rings were cut to avoid the influence of the tool corner radius on cutting forces. Each section of insert edge was used only once, to avoid the effects of wear and workpiece material build-up. The width of cut was 0.35mm, and the feedrate selected was 0.3mm/rev. Under these conditions, the integrity of the tool edge was sometimes lost when cutting with surface speeds above 160m/min, even for the purposes of short cutting force tests. Therefore surface speeds ranged between 10 and 160m/min in these tests. Each test constituted up to 20 revolutions, and acquired data was monitored to check that the length of cut was sufficient for a steady, repeating pattern of cutting forces to be obtained.

Whilst the Dynamometer measurement is a standard approach for obtaining the specific cutting force, the bandwidth of the sensor makes its use for high frequency measurements questionable. Consequently, additional tests performed using a standard shank tool holder (Sandvik RF123K08-2020C) instrumented with an accelerometer, with no dynomometer platform. Modal testing was performed to identify the natural frequencies of the shank tool mounted on the lathe. For these tests, cutting was performed on a Colchester triumph 2000 lathe at feed 0.15mm/rev and width of cut 2mm, to determine the dominant tool vibration frequencies directly from the accelerometer data. This approach was also used to test three tool rake angles, to see the effect on the chip segmentation frequency. Care was taken to avoid excitation of the tool's natural frequencies, thereby ensuring that high segmentation frequencies could be measured without sensor bandwidth issues. This approach was also used to test three different tool rake angles.

3.3 Model validation tests

To test the model predictions, a custom-built flexible toolholder assembly was used in model validation tests [4]. A schematic diagram and photograph of this assembly can be found in Fig. 2. The inserts were held in a Sandvik Coromant blade-style holder, which was welded to a T-shaped monolithic flexure arm. The web of the flexure arm had a cross-section 4.5 by 60mm in the x and y directions of Fig. 2 respectively, which made the assembly much more flexible in the feed (x) direction than in the cutting speed (y) direction. The overhang of the assembly ('OH' on Fig. 2a) was set to 25mm by sliding the flexure arm relative to the base plate, then tightening two large bolts to clamp the arm.

Three transducers were fitted to the toolholder assembly for vibration measurement and modal testing. A Lion Precision eddy current probe sensed the displacement of the flexure arm in the x direction, via a mounted aluminium target. An earth cable was attached to the flexure arm, which resulted in less than $\pm$4mV ($\pm 0.2\mu$m displacement) of noise in the displacement signal with the lathe running. PCB accelerometers were mounted on the flexure arm to measure acceleration in the x and y orientations.

Frequency response functions were obtained for the toolholder and workpiece by applying a modal hammer at the cutting position, and measuring the accelerometers' and probe's response. The receptance of the toolholder and workpiece were recorded, data for the toolholder can be found in Fig. 3. In the x direction,the dominant resonant frequency was 550Hz. Flexibility in the y direction was 100 times lower than in x. Meanwhile, the workpiece was modally tested using the hammer and accelerometer, showing

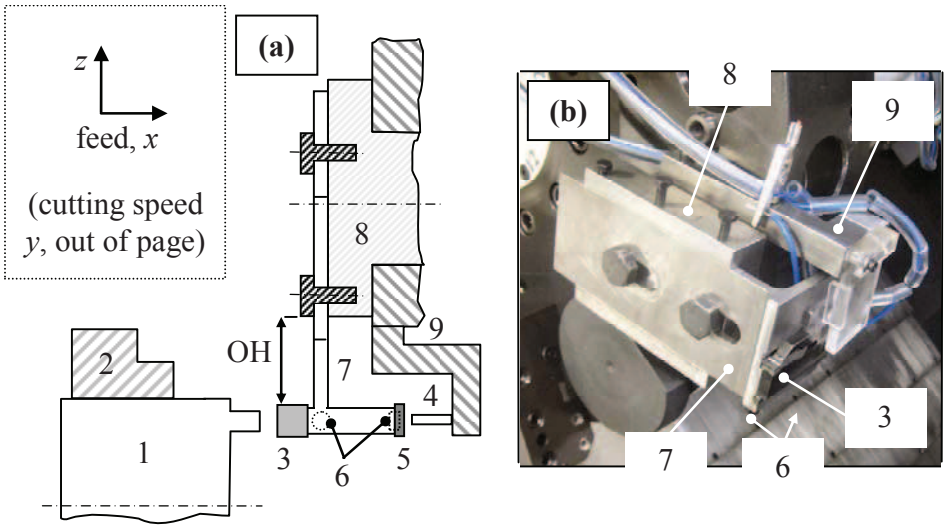

1. workpiece with ring feature
2. lathe chuck
3. cutting insert in blade holder
4. displacement probe
5. aluminium target
6. x, y accelerometers
7. flexure arm
8. base plate, VDI interface
9. turret, probe bracket

Fig. 2 Experimental hardware for turning vibration tests. a) schematic and b) photo.

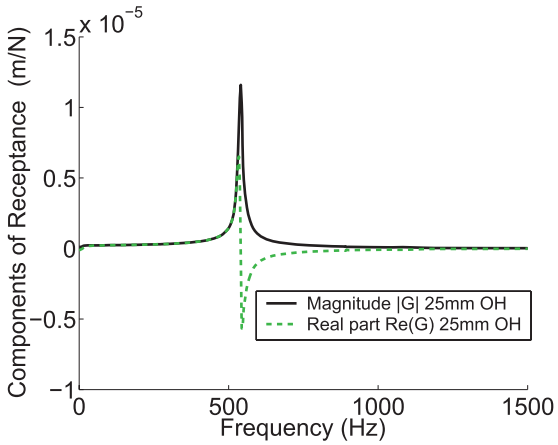

Fig. 3 Receptance frequency response functions, toolholder at 25mm overhang. First 1500Hz shown.

that the maximum flexibility in x was 50 times lower than the toolholder. Consequently, the first mode of vibration of the toolholder in x was by far the most flexible mode of the cutting system.

In the cutting tests, vibration of the toolholder was monitored for a range of cutting parameters: surface speed 10 to 160m/min, feedrate 0.1 to 0.7mm/rev and width of cut 0.35 to 4mm. All cutting was performed orthogonally on rings, with a new section of cutting edge for each test. The accelerometer signals in x and y directions were recorded throughout cutting, as was the probe signal in the x direction. A steady, repeating pattern of vibration displacement against time was achieved in each test.

4 Results

In this section, the empirical data used for model calibration is first presented. Then, a signal processing procedure is described in order to compare model predictions with experimental behaviour. From this analysis, the model's accuracy is summarised.

4.1 Empirical measurements

Section 3.2 described the experimental setup that was used to measure the specific cutting force, along with the chip segmentation forcing frequency and amplitude.

The vibration being studied occurs in the feed direction x, so from the dynamometer data acquired, the steady repeating section of force in the x direction was analysed. Power spectral density (PSD) plots were generated via Welch's method, to see the frequency components in the cutting force and determine the corresponding segmentation frequency.

Fig. 4a shows the segmentation frequency as measured from the x-direction dynamometer measurements. The segmentation frequency is observed to vary with feed and speed. A line of best fit shows that the parameter λ_0 in Eq. (4) is equal to 1.176. Data from the model validation tests are also shown on Fig. 4a, to validate the relationship between segmentation wavelength and chip thickness. Although these results

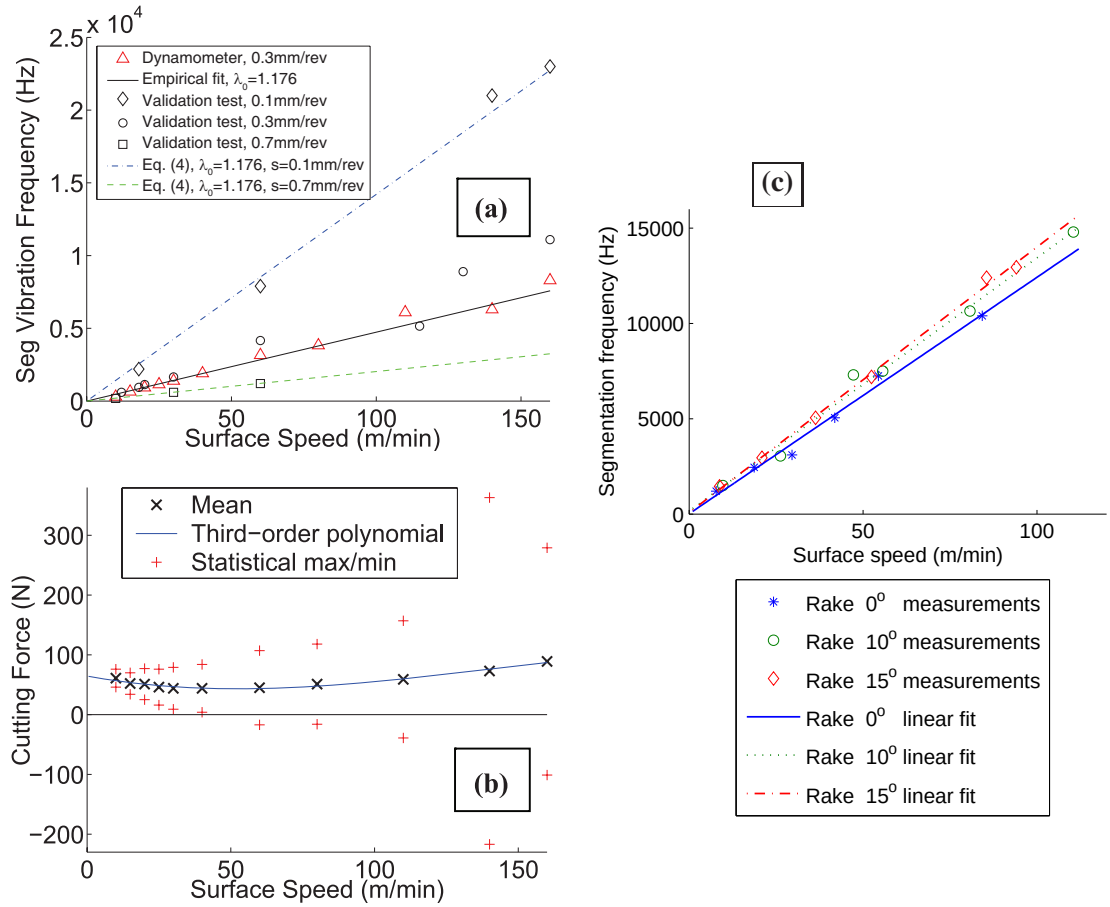

Fig. 4 Model calibration results. a) measured and calculated segmentation-driven vibration frequency; b) measured feed-direction cutting forces against speed, for $b = 0.35$mm and $s = 0.3$mm/rev; c) additional tests using an accelerometer to measure segmentation frequency (b=2mm, $s = 0.15$mm/rev).

will be discussed later, it can be seen that the segmentation frequency is properly predicted by the empirical model given by Eq. (4).

To investigate the cutting forces, the mean value of cutting force was extracted from steady repeating x-direction force data for each test cut. This data is shown in Fig. 4b. A third-order polynomial curve has been fitted to the mean cutting force, giving:

$$\bar{f}_x(V) = -2.4616 \times 10^{-5} V^3 + 0.010329 V^2 - 0.88134 V + 64.565 \tag{13}$$

where $\bar{f}_x$ and V are expressed in N and m/min respectively.

To explore the measured cutting force amplitude, the Hilbert transform was applied to the measured force data so as to obtain the instantaneous amplitude of the signal. This was then plotted as a histogram in order to determine the statistical mode of the periodic amplitude. The 'statistical maximum' was obtained as the mean force plus the mode of the periodic force. The 'statistical minimum' was obtained as the mean force minus the mode of the periodic force. These values are all plotted on Fig. 4b. These maximum/minimum values give an indication of the average range of measured forces for each test.

It can be seen that there is a significant variation in the range of the measured forces. At low speeds, the periodic force (indicated by the red max/min markers) is small compared to the mean (constant) force. This could be due to process damping behaviour which might act to limit the amplitude of the periodic forces at lower speeds. In any case, at the lowest surface speeds the frequencies associated with this periodic force are within the measurement capabilities of the dynamometer and so this suggests that the periodic forces are at least 5 times smaller than the mean force in this region.

However at high speeds the periodic force becomes greater than the mean force, which suggests that the cutting force becomes negative during some parts of each vibration cycle. This may seem counter-intuitive, but it should be pointed out that the frequency of these periodic forces is up to 25kHz - way beyond the first natural frequency of the dynamometer. Consequently, Fig. 4b serves to illustrate the problems associated with quantitative measurements of the chip segmentation forces, but does not help to accurately determine the value of Δf_x in Eq. (6). With reference to Eq. (7) the value of n appears to be greater than 5 based upon the low surface speed measurements.

Results from the additional calibration tests are plotted in Fig. 4c. Here, three different rake angles are shown, to illustrate that the segmentation frequency is only moderately sensitive to this tool geometry. In addition, the data was obtained using an accelerometer rather than the dynamometer. Comparing Fig. 4a and c, the similar behaviour demonstrates that the dynamometer was still able to predict the segmentation frequency, even if the dynamometer amplitude could not be trusted at higher frequencies.

To summarise, the empirical approach has allowed the specific cutting force (Eq. (8)) to be identified as a 3rd order polynomial (Eq. (13)), whilst the segmentation wavelength coefficient (Eq. (4)) is 1.176 for the 7° rake tool (Fig. 4a). As expected the amplitude n of the mean cutting force to the periodic cutting force (Eq. (7)) is not easily measured but appears to be more than 5, based upon low speeds where more accurate measurements are possible.

4.2 Model validation tests

The empirical data allows Eq. (10) to be used to predict the vibration amplitude when machining with a flexible workpiece or tool. To validate this, a flexible toolholder was designed and tested as described in Section 3.3. A set of data processing functions were used to extract frequency and amplitude information from the toolholder displacement measurements. Fig. 5 illustrates the displacement data processing methods and presents a photo of some interesting cases. Power spectral density (PSD) plots were created, to see the frequency components in each displacement signal. The Hilbert transform was then used to extract the instantaneous vibration amplitude. This was then plotted on a histogram to find the statistical mode of vibration amplitude, a_{mod}. Three examples of displacement data versus time are shown in Fig. 5b, with the resulting PSD plots, and amplitude histograms with the mode values marked.

Classification of vibration requires that a boundary value be set, beyond which the level of vibration is unacceptable. In practice, the boundary value is usually chosen according to the specification for the

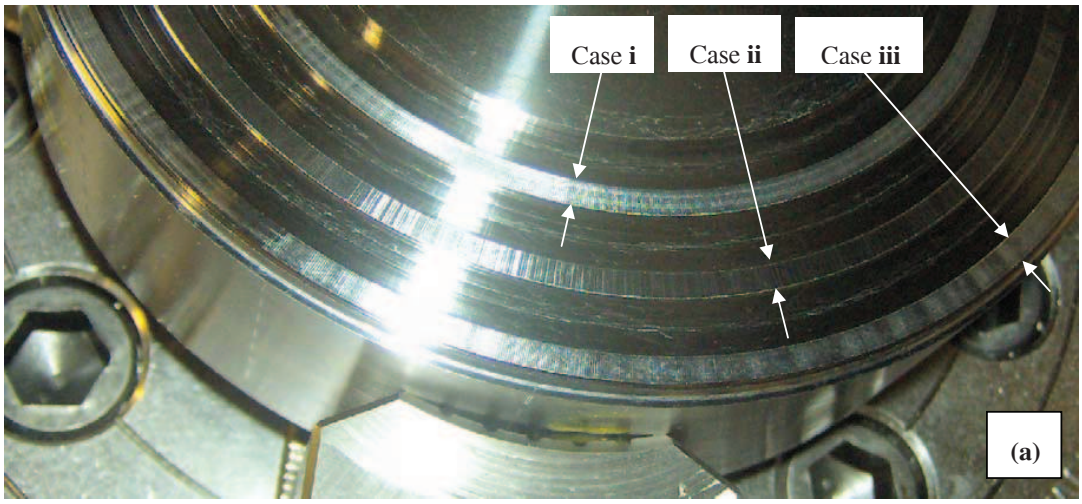

Cases **i**, **ii** and **iii** featured above, cases **ii**, **iii** and **iv** featured below. All cases featured in Fig. 7

Case **i** not featured below: V=75m/min, b=3mm, s=0.4mm/rev, a_{mod}=3.8 μm

Case **ii**: V=32m/min, b=3mm, s=0.4mm/rev

Case **iii**: V=65m/min, b=3mm, s=0.4mm/rev

Case **iv**: V=16m/min, b=0.6mm, s=0.4mm/rev

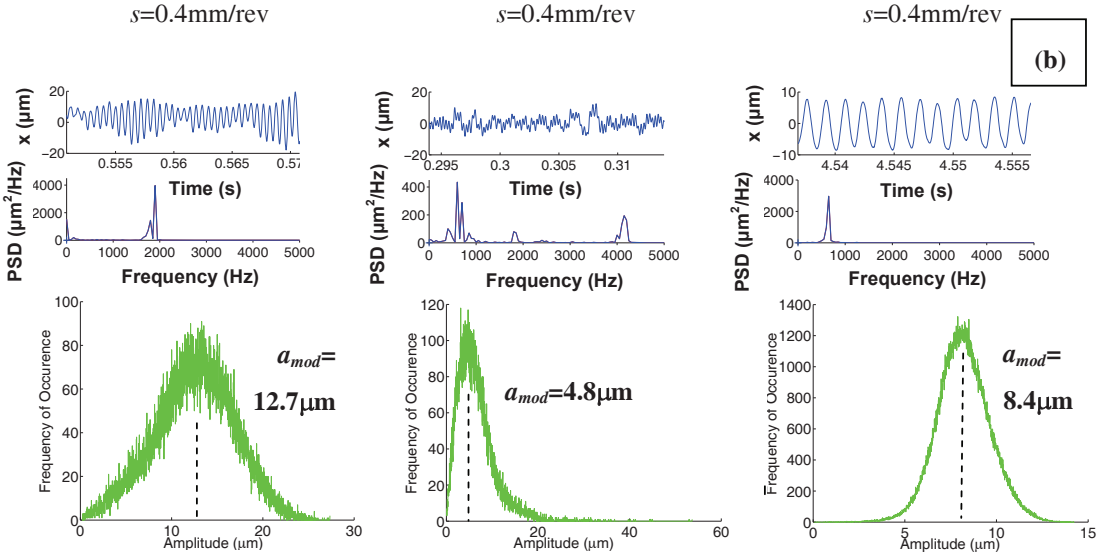

Fig. 5 Example test results. a) surface finish after cutting and b) typical data analysis

machined part. In this work, the condition for excessive vibration is based on a_{mod} being equal to or greater than 5μm. Where a_{mod} is in the range 4.5 to 5μm, vibration is considered borderline. Case **iii** in Fig. 5a shows the surface finish for what is considered a borderline-acceptable (a_{mod} 4.8μm) cut.

Three interesting vibration examples have been selected for examination in Fig. 5b. The top row of plots shows the displacement signal against time, the middle row of plots shows frequency components from the PSD analysis, and the bottom row shows a vibration amplitude histogram derived using the Hilbert transform. In case **iv**, a high level of vibration occurred at a relatively low width of cut and surface speed, due to excitation of resonant vibration. This result agrees well with the model predictions, since the segmentation frequency is close to the natural frequency of the toolholder. In case **iii**, borderline acceptable vibration

occurred at a relatively high width of cut and surface speed. Multiple frequency components are present in the PSD plot, but it should be noted that the amplitude of these vibrations is quite small. In case **ii**, segmentation vibration was expected to occur at 1.13 kHz, but the vibrations occurred at a frequency of approximately 1.8-2kHz. This is an example which is not predicted accurately by the model.

Returning to Fig. 4a, PSD results from the model validation tests have been included using data for feedrates of 0.1, 0.3,and 0.7 mm/rev. This serves to demonstrate that the observed segmentation frequency generally matches the trends predicted by Eq. (4), despite the behaviour observed for case **ii**.

The results of vibration amplitude analysis indicate that in no case did the tool leave the cut due to vibration, as required for assumption (b) made in Section 2.1. In all cases, the maximum vibration amplitude was less than half of the uncut chip thickness.

The validity of Eq. (12) is explored in Fig. 6a. Here, three tool geometry and feed scenarios are presented. A tool relief angle of 7° leads to a larger clearance between the tool and the just-cut surface, so that Eq. (12) predicts a larger vibration amplitude (a_{max}) before interference starts to occur. This amplitude is proportional to the feed rate s so a lower a_{max} is expected for a feed of 0.4 mm/rev compared to 0.5 mm/rev. Changing the relief angle to 3.5° results in an even lower a_{max}. The experimental data show that at low surface speeds all three test conditions cause high vibration amplitudes. In each case the vibration amplitude becomes limited at a value close to that predicted by Eq. (12). Given the approximations involved in Eq. (11) and (12), in particular the assumption of no interference or ploughing, the agreement between observed and predicted behaviour is good.

At higher surface speeds the observed vibration amplitude becomes smaller. This can be explained by Eq. (10), but as previously mentioned, the value of the n is difficult to quantify. Using a value of $n = 8$ leads to model predictions that are close to the experimentally observed behaviour, as shown in Fig. 6b.

To summarise, the results so far have suggested that the amplitude of vibration can be predicted by a combination of forced vibration due to chip segmentation, and tool-flank interference (which limits the maximum amplitude). The frequency of the forced vibration due to chip segmentation (Fig. 4a) can be predicted reasonably well from empirical data, which agrees with previous findings [15, 18]. However, the amplitude of vibration is more difficult to quantify because it is difficult to measure the periodic component of the cutting force for empirical calibration purposes.

Despite this drawback, it transpires that a relative prediction of vibration amplitude is still possible. For lightly damped structures the vibration amplitude increases so drastically around the resonant frequencies that regions of high amplitude vibration can be easily identified based upon Eq. (10), even when the parameter n is not accurately known. Before illustrating this, a classification method will be introduced so that all of the experimental data can be categorised.

4.3 Classification and summary of results

The experimental vibration data was classified according to the following criteria:

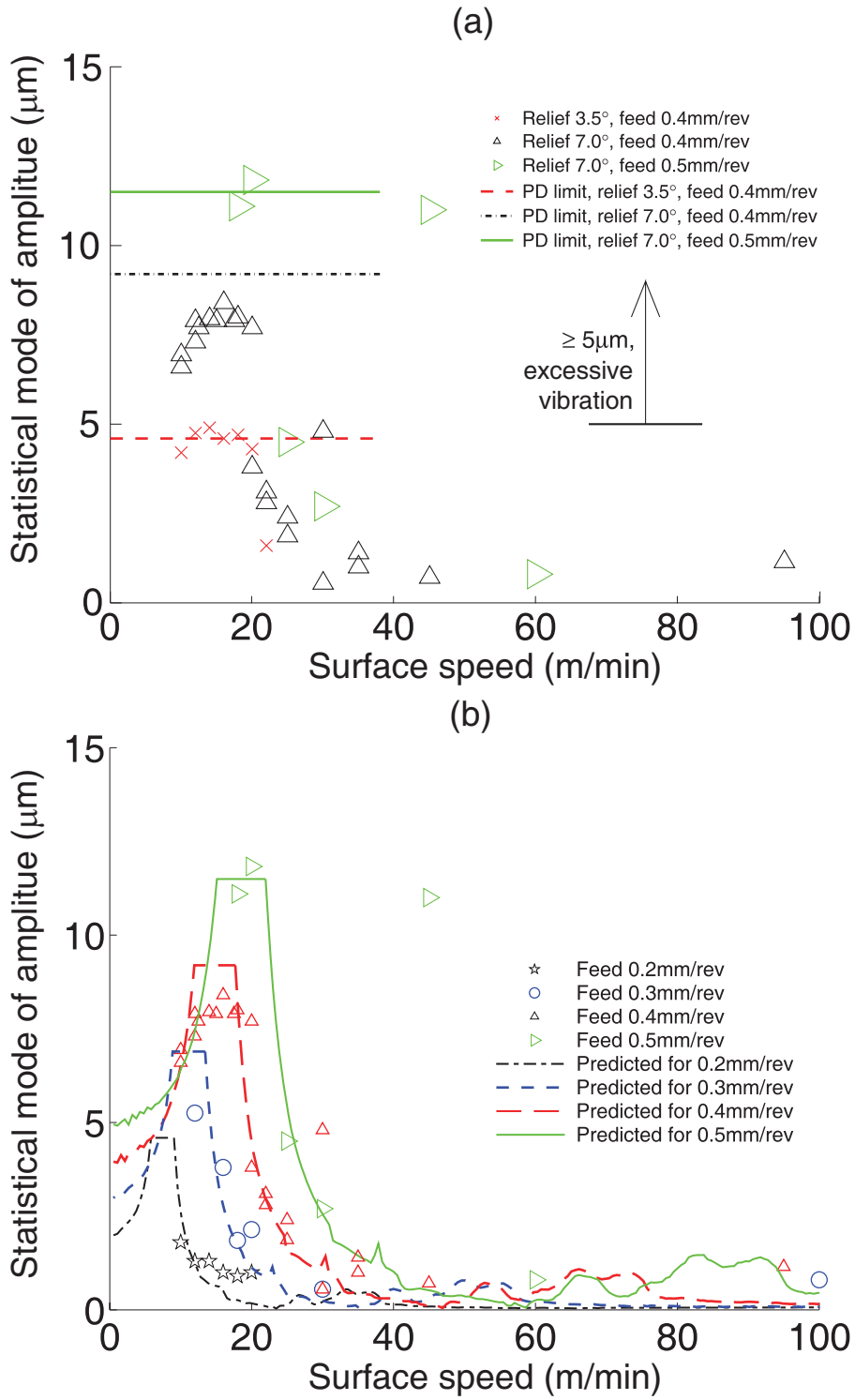

Fig. 6 Cutting test data compared to model predictions for width of cut $b = 0.6$mm. a) comparison against process damping amplitude limits predicted by Eq. (12) for three example feed rates / geometries; b) comparison against predicted segmentation and process damping amplitudes (Eq. (10) and (12)) for four example feed rates, using $n = 8$ in Eq. (10).

1. When the mode of the vibration amplitude was below 4.5μm the cut was classified as 'acceptable'.
2. When the mode of the vibration amplitude was between 4.5μm and 5.0μm the cut was classified as 'borderline'.
3. When the mode of the vibration amplitude was above 5μm the cut was classified as follows:
   (a) Where the PSD showed a dominant frequency between 550 and 600 Hz the cut was classified as 'regenerative chatter'. This classification was based upon the study described in [4], which used the same flexible toolholder configuration.
   (b) Where the PSD showed a dominant frequency within 15% of that predicted by Eq. (4) the cut was classified as 'segmentation-driven vibration'.
   (c) Where neither of these was the case, the cut was deemed 'Unclassified'.

Note that with this classification, there is a small region where both 3(a) and 3(b) can be satisfied simultaneously. This occurs when the frequency of forced vibration due to chip segmentation is very close to the minimum in the real part of the receptance FRF (Fig. 3). Under such conditions it becomes impossible to distinguish between segmentation and regenerative vibrations.

Results for a feed rate of 0.4 mm/rev are displayed in Fig. 7. To simplify the illustration, predicted amplitudes are based solely on Eq. (10), rather than including the process damping behaviour from Eq. (12). It can be seen that the cuts classified as 'segmentation-driven vibration' are all concentrated within a small region of the figure. This coincides with a high amplitude predicted from Eq. (10). On Fig. 7, the calibration coefficient n is set to unity (i.e. the peak amplitude of the periodic force is assumed equal to the mean force). This results in predicted amplitudes that are 5-10 times higher than the experimentally observed behaviour. However, the result is still useful from a machining process design perspective. From the point of view of choosing appropriate speeds and widths of cut, it is quite clear from Fig. 7 that higher surface speeds are needed ($>$30 m/min) if a high width of cut is required, whilst lower speeds ($>$20m/min) can be used if the width of cut is very small.

This form of presentation suffers from the drawback that as the feed rate is changed, the predicted regions of high vibration magnitude will move, because the segmentation frequency changes. In contrast, Eq. (10) predicts a linear relationship between vibration amplitude and width of cut b. This makes it more appropriate to plot the predicted amplitude in terms of the surface speed and the feed rate. Such a result is shown in Fig. 8, for a width of cut of $b = 0.6$mm. It should be reiterated that the calibration coefficient n is not known, and therefore the vibration amplitude is only predicted in relative terms. Meanwhile, because the amplitude is proportional to the width of cut, the shape of the vibration amplitude contours will be unaffected by changes in the width of cut. This makes Fig. 8 a more effective way to illustrate the predicted regions of high amplitude vibration.

To summarise the experimental validation, 25 of 68 test cuts exhibited high amplitude vibration, and in 16 of these cases, the main cause was concluded to be chip segmentation, which can be predicted by the model.

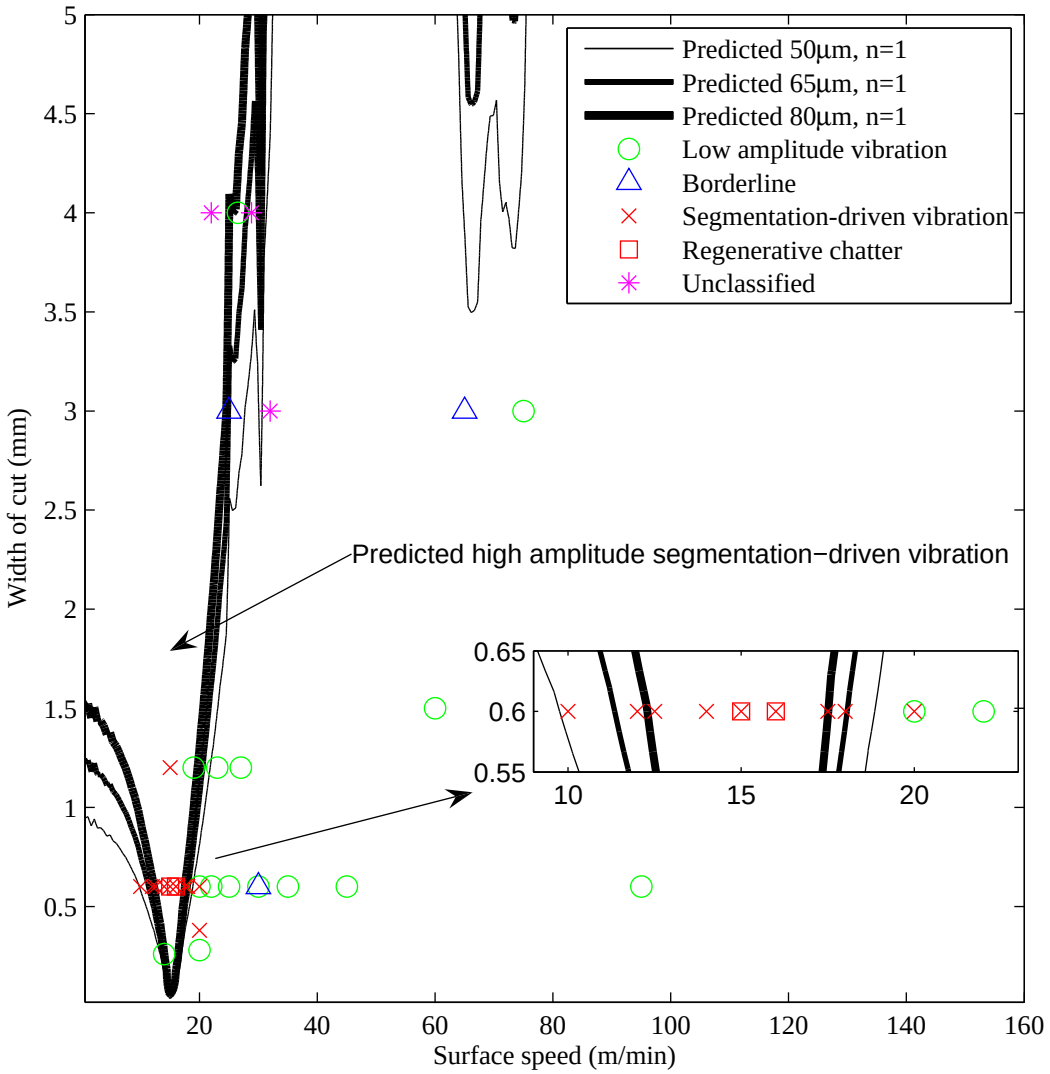

Fig. 7 Model validation: width of cut versus speed, feed rate $s = 0.4$mm/rev. A close-up of the data around $V = 15$m/min, $b = 0.6$mm is included.

5 Discussion

A number of points are worthy of further discussion at this stage.

First, the experiment data can be compared to previous literature where the segmentation effect has been observed. In comparison to the data of Sun *et. al* [18] who also performed dry turning of Ti6Al4V, the equivalent chip segmentation wavelength coefficient is a factor of three from that found in the current work. This could be due in part to the chip thinning effect from a 45° side cutting edge angle. Other material and tool parameters may also be significant. A different form of Eq. (4) might be required where the surface speed changes over several orders of magnitude [16], but for typical applications, a linear relationship is sufficient.

It should be noted that in the present study, a controlled experiment was performed to validate the model. This involved the design of a flexible tool holder that was very stiff in the y (surface speed) direction.

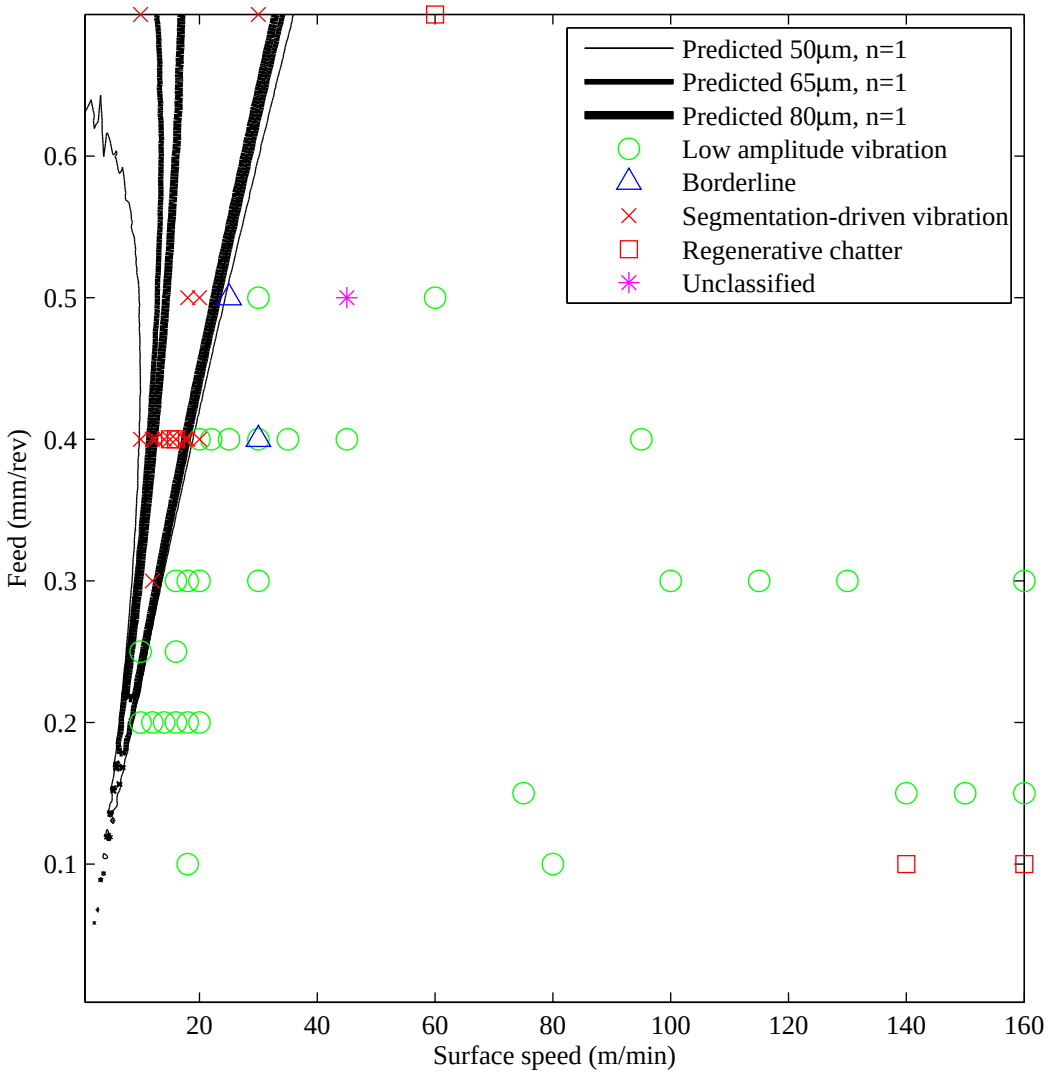

Fig. 8 Model validation: feed versus speed, width of cut $b = 0.6$mm.

However, the modelling approach could be readily extended to consider vibration in other orientations. This will be the subject of further work.

Finally, based on findings of this work, some recommendations for industrial practice can be made. To acheive low vibration and high productivity in turning Ti6Al4V, standard practice would be as follows:

- work in a high-speed machining stability lobe, to select a width of cut below the regenerative chatter stability limit or,
- work in the low-speed process damped region to avoid regenerative chatter.

The present results suggest that this latter approach could be less effective unless chip segmentation behaviour is properly considered. In particular, Fig. 8 shows that even without a quantitative prediction of vibration amplitude, suitable feed rates and surface speeds can be selected so as to avoid segmentation driven vibration, whilst still operating within a process damped region to enhance regenerative chatter stability.

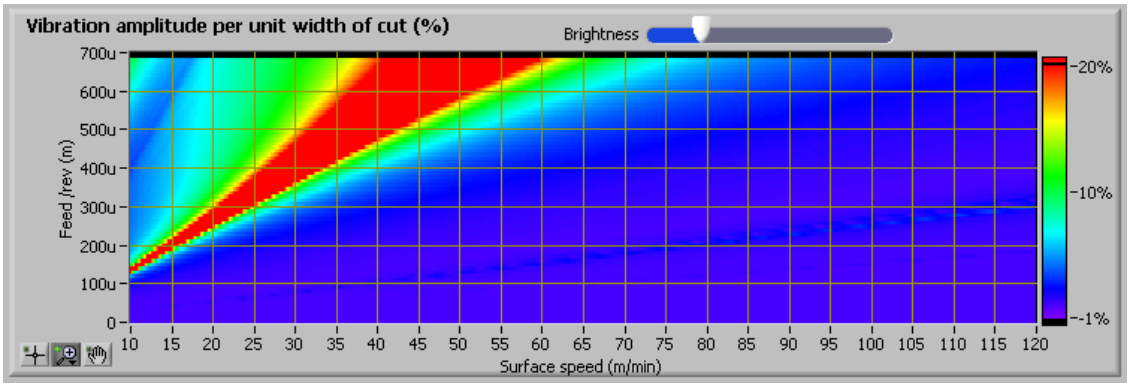

Fig. 9 Example LabVIEW graphical user interface for illustrating regions of segmentation-driven vibration.

This is further illustrated in Fig. 9, which shows an equivalent figure created using prototype commercial software, programmed in LabVIEW[22].

6 Conclusions

The present study has proposed a methodology for predicting the onset of high-amplitude vibrations due to chip segmentation effects. This undesirable behaviour has been referred to as segmentation-driven vibration. It has been demonstrated that the pattern of behaviour for segmentation-driven vibration can be predicted, given empirical measurements that are similar to those required for classical regenerative chatter. Furthermore, it has been shown that at some surface speeds the maximum vibration amplitude becomes limited due to process damping behaviour, and this level of vibration agrees well with the approach proposed by Hooke and Tobias [8].

The chip segmentation model was verified via turning tests on titanium Ti6Al4V alloy. A total of 68 cuts were made and the 16 cases of segmentation-driven vibration all occurred within or adjacent to the predicted region. In order to quantitatively predict the vibration amplitude, a greater understanding is required of the periodic cutting forces during segmented chip formation. This requires novel experimental approaches [10] since standard dynamometers are ineffective at the higher frequencies sometimes required. Despite this drawback, the present contribution has demonstrated that segmentation-driven vibration can be predicted satisfactorily for the purposes of machining process design. In addition, this prediction can be acheived with the standard measurement equipment that is used for regenerative chatter analysis.

Acknowledgements

The authors are grateful for the support of the EPSRC, through grant reference EP/D052696/1. Thanks to Mr Jamie Booth, for his technical assistance with the manufacture of the flexible toolholder.

References

1. J. Tlusty and M. Polacek. The stability of the machine tool against self-excited vibration in machining. *Proc. Int. Res. Prod. Eng.*, pages 465–474, 1963.
2. J. Tlusty. *Manufacturing Processes and Equipment*. Prentice Hall,, New Jersey, USA, 1999.

3. R. Komanduri and B. F. Von Turkovich. New observations on the mechanism of chip formation when machining titanium alloys. *Wear*, 69:179–188, 1981.
4. C. M. Taylor, S. Turner, and N. D. Sims. Chatter, process damping and chip segmentation in turning: a signal processing approach. *J. Sound Vib*, 329(23):4922–4935, 2010.
5. E. Budak and L. T. Tunc. A new method for identification and modeling of process damping in machining. *Journal of Manufacturing Science and Engineering*, 131(5):051019–10, 2009.
6. M. Eynian and Y. Altintas. Chatter stability of general turning operations with process damping. *Journal of Manufacturing Science and Engineering*, 131(4):041005–10, 2009.
7. A.R. Yusoff, S. Turner, C.M. Taylor, and N.D. Sims. The role of tool geometry in process damped milling. *International Journal of Advanced Manufacturing Technology*, 50(9):883–895, 2010.
8. C. J. Hooke and S. A. Tobias. Finite amplitue instability- a new type of chatter. In *Proc. 4th Int. M.T.D.R. Conf., Manchester UK*, pages 97–109, 1963.
9. D. W. Wu. Application of a comprehensive dynamic cutting force model to orthogonal wave-generating processes. *Int. J. Mech. Sci.*, 30(8):581–600, 1988.
10. A. Vyas and M. C. Shaw. Mechanics of saw-tooth chip formation in metal cutting. *J. Manuf. Sci. Eng.*, 121:163–172, 1999.
11. S. Kalpakjian and S. Schmid. *Manufacturing Engineering and Technology*. Pearson Educations, New Jersey, USA., 2006.
12. N. H. Cook. Chip formation in machining titanium. In *Proc. Symp. Machining and Grinding Titanium, Watertown, MA, USA*, pages 1–7, 1953.
13. P. Landberg. Vibrations caused by chip formation. *Microtechnic*, 10(5):219–228, 1956.
14. S. Jeelani and K. Ramakrishnan. Surface damage in machining titanium 6al-2sn-4zr-2mo alloy. *J. Mater. Sci.*, 20:3245–3252., 1985.
15. A. E. Bayoumi and J. Q. Xie. Some metallurgical aspects of chip formation in cutting ti-6wt. *Mater. Sci. Eng.*, A190:173–180., 1995.
16. A. Molinari, C. Musquar, and G. Sutter. Adiabatic shear banding in high-speed machining of ti6al-4v: Experiments and modeling. *Int. J. Plasticity*, 18:443–459, 2002.
17. A. K. M. Nurul Amin, A. F. Ismail, and M. K. Nor Khairusshima. Effectiveness of uncoated wc-co and pcd inserts in end milling of titanium alloy- ti-6al-4v. *J. Mater. Process. Technol.*, 185:147–158, 2007.
18. S. Sun, M. Brandt, and M. S. Dargusch. Characteristics of cutting forces and chip formation in machining of titanium alloys. *Int. J. Mach. Tools Manuf.*, 49:561–568, 2009.
19. M. Doi and M. Ohhashi. A study on parametric vibration in machining of hard cutting metals. *Int. J. Japan Soc. Prec. Eng.*, 26(3): 195–200., 1992.
20. M. D. Morehead, Y. Huang, and J. Luo. Chip morphology characterization and modeling in machining hardened 52100 steels. *Machining Science and Technology*, 11(3):335–354, September 2007. ISSN 1091-0344. URL `http://www.tandfonline.com/doi/abs/10.1080/10910340701567289`.
21. G. Stepan. Modelling nonlinear regenerative effects in metal cutting. *Philosophical Transactions of the Royal Society of London, Part A*, 359:739–757, 2001.
22. C. M. Taylor and N. D. Sims. A method to minimise vibration in the machining of hard, segmenting metals. UK patent application, 2010.

a_x	vibration amplitude in feed direction x
a_{max}	limit value of a due to process damping
a_{mod}	statistical mode value of a
b	width of cut
b_{lim}	maximum stable width of cut
ω_c	chatter frequency
ω_{seg}	segmentation frequency
$f_x(t)$	instantaneous cutting force in x direction
$\bar{f}_x$	average (mean) value of $f_x(t)$
Δf_x	peak amplitude of oscillation of $f_x(t)$
$G(\omega)$	x direction receptance frequency response function
K	specific cutting force in x direction
n	vibration amplitude calibration coefficient
s	feedrate (feed per rev)
V	surface speed
x	displacement in feed direction
α	tool relief angle
λ	chatter wavelength
λ_0	segmentation wavelength coefficient

Nomenclature